# *Elaboration and thermal annealing of the optical properties of the thin films of meta-PPV copolymer*

**S. M. Ahmad**

**Polymer Bulletin**

ISSN 0170-0839

Polym. Bull.
DOI 10.1007/s00289-018-2655-9

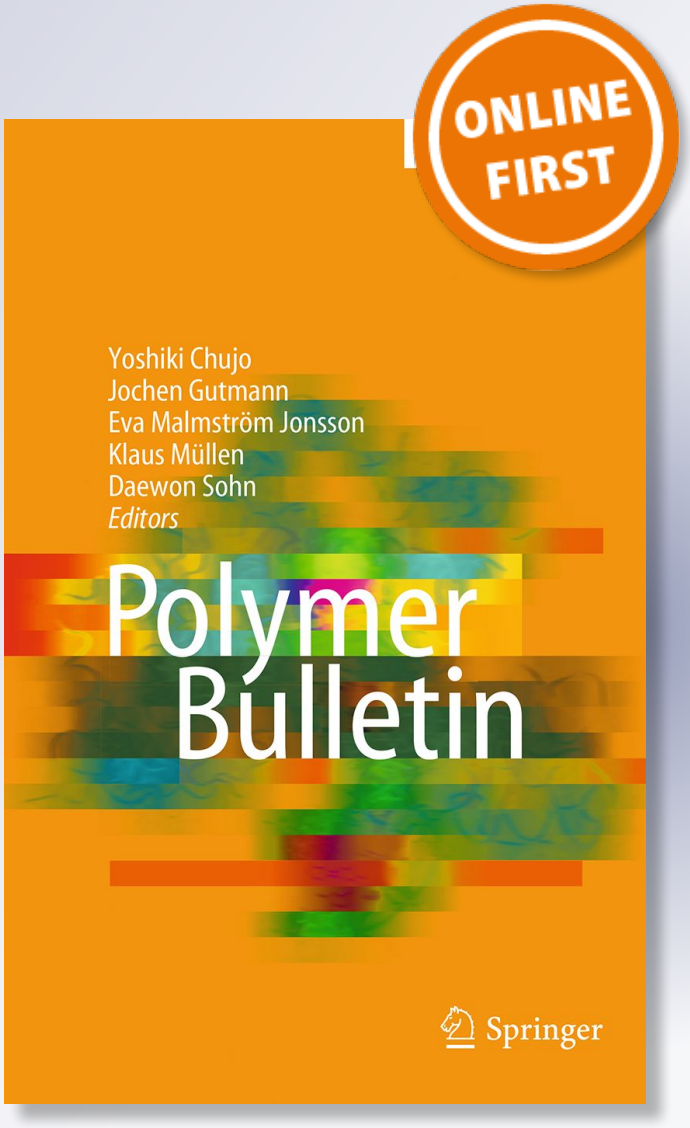


Springer

Polymer Bulletin
https://doi.org/10.1007/s00289-018-2655-9

ORIGINAL PAPER

# Elaboration and thermal annealing of the optical properties of the thin films of meta-PPV copolymer

**S. M. Ahmad**[1]

Received: 4 August 2018 / Revised: 4 October 2018 / Accepted: 7 December 2018


## Abstract

The meta-PPV copolymer was prepared by the condensation of the diphosphonium chloride of meta-xylene with dialdehyde of vanillin. Meta-PPV thin films were successfully deposited on glass substrates by spin casting method. The polycrystalline structure of the films was confirmed using X-ray diffraction (XRD) analysis, and also XRD was utilized to compute the grain size and dislocation. Surface morphology was characterized by using photomicroscope and scanning electron microscopy. Fourier-transform infrared spectroscopy was used to verify the presence of the absorbance bands. The optical absorption measurement revealed direct-allowed electronic transition with band gaps 3.3 eV and 2.85 eV for as-deposited and annealed films, respectively. The redshift of the band gap and related optical constant after annealing was assigned to the change in configuration and conformation of copolymer chains. Thermal annealing leads to the reduction in PL efficiencies and redshift of single peak which attributed to band-to-band transition.

**Keywords** Meta-PPV · Thin film · Optical properties · Thermal annealing · XRD

## Introduction

Conducting polymers such as PPV and its derivatives were the promising future of organic electroluminescent materials [1]. In particular, conjugated polymer thin films achieved extensive interest among scientists over the past two decades because of their versatility and ease of preparation [2]. Since the discovery of electroluminescent poly(phenylene vinylene) PPV in 1990 [3], PPV continues to receive enormous interest for application in optical and electronic devices such as organic light emitting diodes (OLED) [4], field effect transistors (FETs) [5] and solar cells [6]. PPV is a highly stable conjugated polymer; the small optical band gap (2.5) eV and its bright yellow fluorescence make it nominated for many

✉ S. M. Ahmad
smahmood42@yahoo.com

[1] Physics Department, College of Science, University of Basrah, Basrah, Iraq

Published online: 13 December 2018

applications [7]. Significant researches have been achieved to study the band gap of conjugated polymers through changes in chemical structures [8], as always important for conducting polymer, the ability to influence the band gap in the molecules predictable fashion, so that their electronic properties can be tuned to match the desired application [9]. By the inclusion of different functional side groups, the physical and electronic properties of PPV derivatives can be modified.

Although PPV is one of the best polymer materials to be used as an efficient accepter in polymeric solar cell, its structure causes low solubility and aggregation as it is insoluble in pure form because of the high dielectric mismatch with conventional solvents; this intractability can be overcome either by involvement of chemically attached side chains to the polymer backbone, as the side chains produce an organic layer surrounding the polymer backbone to increase the compatibility of the polymer with organic solvents [10] or by introducing flexible non-conjugated spacers into the polymer backbone [11]. The synthesis of conjugated soluble electroluminescent polymer by using PPV with long alkyl or alkoxy ramification was the first approach used [12]. Oriented PPV was found to be mechanically strong, highly crystalline and environmentally stable [13, 14]. Several methods for synthesis of PPV have been reported [15–17], but chemical method is one of the easiest. The structural and hence the optical properties vary dramatically, based on which precursor polymer utilized [18], and the prepared PPV by this method had better chain ordering resulting in larger modifications in the electronic structure [19]. Conjugation confinement can be achieved by tailoring the polymer structure via inserting (para, meta, ortho) linkages or imposing steric distortions.

Xylene is an aromatic hydrocarbon that exists in three isomeric forms. The isomers can be distinguished by the designations ortho (o-), meta (m-) and para (p-) which specify to which carbon atoms (of the benzene ring) the two methyl groups are attached. Of the three isomers, the meta-xylene (1,3-dimethyl benzene) is rarely sought and it is used in the manufacture of isophthalic acid which is in turn used as a copolymerizing monomer hence the utility of its conversion to the p- and o-isomers [20]. To our knowledge, there are no previous studies that have been carried out on (meta-PPV) thin films. In this study, the m-xylene was used to synthesize copolymer thin films under term conjugated-non-conjugated copolymer because of the presence of aliphatic spacer between aromatic rings. The copolymer contains alkyl group ($CH_3$) in the position meta, and the presence of this group with aliphatic spacer leads to the variation in the energy band gap and affected the photoluminescence (PL) efficiency.

Thermal annealing of polymer can play a very important role in changing the physical properties; if annealing temperature is greater than the temperature glass transition ($T_g$), the polymer chains will relax [21]. In this study, the samples are annealed at 200 °C (greater than $T_g$ which is around 80 °C) for 1 h; so in this article, the effect of meta-linkage in the main chain of the optical and structural properties of the copolymer thin film will be studied; moreover, the effect of thermal annealing on the optical constant was estimated.

The as-deposited films were investigated by X-ray diffraction (XRD), scanning electron microscopy (SEM), photomicroscope, Fourier-transform infrared spectroscopy

(FTIR), ultraviolet–visible (UV–vis) absorption spectrophotometer and photoluminescence spectra (PL). All measurements were taken at room temperature.

## Experimental process

### Chemicals

Meta-xylene, acetone, chloroform, sebacyl chloride and vanillin were supplied from Fluka, while triphenyl phosphine, concentrated hydrochloric acid 36%, formalin solution 35%, absolute ethanol and sodium metal were supplied from Merck Company. These materials were used without further purification.

### Preparation methods

#### Synthesis of 2,4-bis (Chloromethyl) m-xylene [I]

In a round-bottom flask size 250 ml, 0.094 mol from p-xylene, 0.1 mol formalin solution (35%) and 105 ml concentrated hydrochloric acid (37%)were mixed together and refluxed for 5 h at the end of the reaction time, cooling the product and converting the reaction mixture into large beaker and storing in a cool place for 24 h. The white precipitate was collected and washed several times with water to remove the remaining acid and then washed with methanol, filtrate and dried under vacuum to give white solid product, with m-point 95 °C and yield 81%.

#### Preparation of phosphonium salt of compounds [II]

0.2 mol from compound [I] and 0.2 mol from triphenyl phosphene were dissolved in 50 ml xylene, and the mixture was refluxed for 24 h; solid product was precipitated and filtrated after cooling the reaction, washed twice with xylene and finally with acetone to give white product yield 85%. The same procedure was performed for the preparation of the phosphonium salt of compound [II]

#### Synthesis of dialdehyde compound [III[

0.21 mol of vanillin was mixed gently with 0.1 mol of 1,4-di bromo butane, and the mixture was heated at 80 °C with stirrer in the presence of 10% potassium hydroxide for 2.5 h; after cooling, slight yellow powder was the product, then the remaining of acid was neutralized with sodium bicarbonate, and finally the chloroform layer was isolated and evaporated in order to get the slightly yield yellow product.

#### Synthesis of polymer [IV]

Equal amounts of compound [II] and [III]were dissolved in 50 ml ethanol/chloroform mixed solvent (3/1 ratio), then 10 ml from absolute alcohol containing 0.63 mg

sodium metal was added dropwise with good stirring under room temperature. After complete addition, the reaction mixture was kept 24 h at room temperature, then 2% hydrochloric acid solution was added, and the polymer was isolated as viscous brown product was characterized by FTIR analysis (Scheme 1).

## Results and discussion

### Structural properties

#### XRD analysis

The structure of the films was characterized by X-ray diffraction using CuKα radiation ($\lambda = 1.548$ Å), and the mean diameter (D) of the grain size of meta-PPV derivatives thin films was calculated using Sheerer formula [22].

$$D = 0.9\lambda/\beta \cos\theta \tag{1}$$

where $\theta$ is Bragg angle and $\beta$ is the experimentally observed diffraction peak width at full wave half maximum intensity (FWHM). The value of dislocation was equal

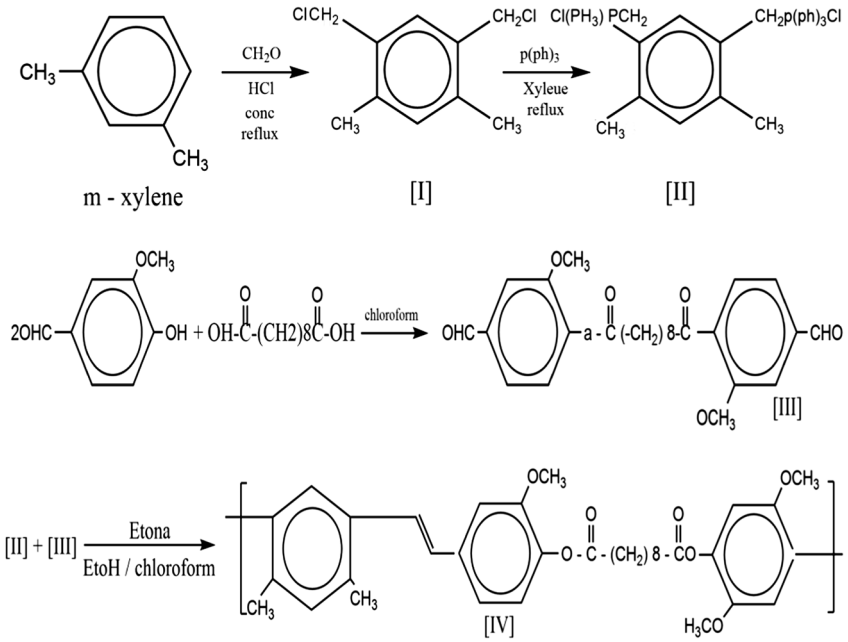


Ploy [(4,6) – dimetlyl)1.3 phenylene vinylene -3- methpxy 1.4 phernylene 1.10 – dioxy decametlylene 2- methoxy 1.4 phenylene

**Scheme 1** Route of prepared copolymer

to $(2.3 \times 10^{-4}(\text{nm})^{-2})$ of m-PPV thin films representing the amount of defect in the crystal structure, obtained by applying the relation $\delta = 1/D^2$.

The structure of PPV has been extensively studied. Since it is typically prepared during thermal conversion of highly processible precursor polymer, it is possible to control the degree of crystalline order and film morphology [23, 24]. The main feature of the diffraction pattern of m-PPV thin film was polycrystalline nature as shown in Fig. 1; three peaks observed are represented by miller indices (110), (200) and (210) planes corresponding to $2\theta = 22.1$, $2\theta = 23.6$ and $2\theta = 29.3$ which were close to the reported [25]. When comparing the XRD pattern of our study with others [26], an increase in the number of peaks can be seen, the behavior can be attributed to the increase in the heterogeneity of the film to host lattice occupation by m-linkage and to the decrease in the crystalline sizes to nanolevels (65 nm) since inserting meta-linkage disrupts the crystalline order of m-PPV films and has a significant influence in the disordering of polymer chain [27].

The highest peaks were around the (200) plane and were in good agreement with that reported elsewhere [26] which confirm PPV formation. Since the XRD and miller indices for m-PPV are rare, we cannot mention all miller indices of other angles that appeared.

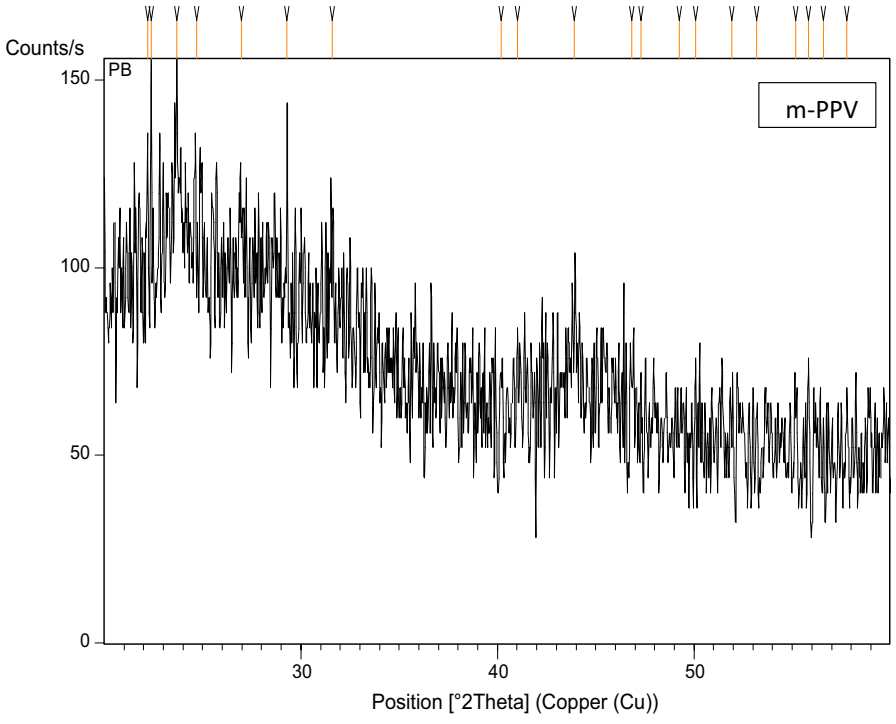


**Fig. 1** X-ray diffraction spectra of m-PPV thin film

## FTIR analysis

IR absorption wildly characterizes the interactions between the vibration energy of bonds and electromagnetic waves [28], and it is used to verify the quality of the cast films as well as for any shift in the absorbance bands. The prepared copolymer was characterized by using Fourier-transform infrared (FTIR) at the (400–4000) $cm^{-1}$ region using the KBr solution. As seen in Fig. 2, we observed the absorption band of the copolymer at the region 3070 $cm^{-1}$ due to CH=CH stretching (along the vinyl band) copolymer chain. However, the absorption band at the region 1720 $cm^{-1}$ corresponds to the carbonyl group and along the copolymer chain. Finally, the absorption band around 1600 $cm^{-1}$ is due to aromatic benzene.

## Surface morphology analysis

The morphology of the spin-coated polymer thin film is an important factor in fabrication polymer solar cells. To obtain more information on surface structural features of the films, photomicroscope image and SEM for samples were achieved. Figure 3 shows a spherical structure composite of nanoparticle, and it reveals good homogeneity and full coverage of the copolymer on the glass substrate. There are no foreign objects on the surface or pieces that are completely insoluble; moreover, the films look yellowish green. In order to characterize the surface structural of the m-PPV thin film, SEM image of three magnifications was achieved, as shown in Fig. 3. At a scale of 100 µm, the vicinity of the surface is homogenous and no such irregular objects were seen with good quality on glass substrate adhesion. The film revealed a porous structure, unless there is some aggregation which is caused by interpenetration of adjacent chain in

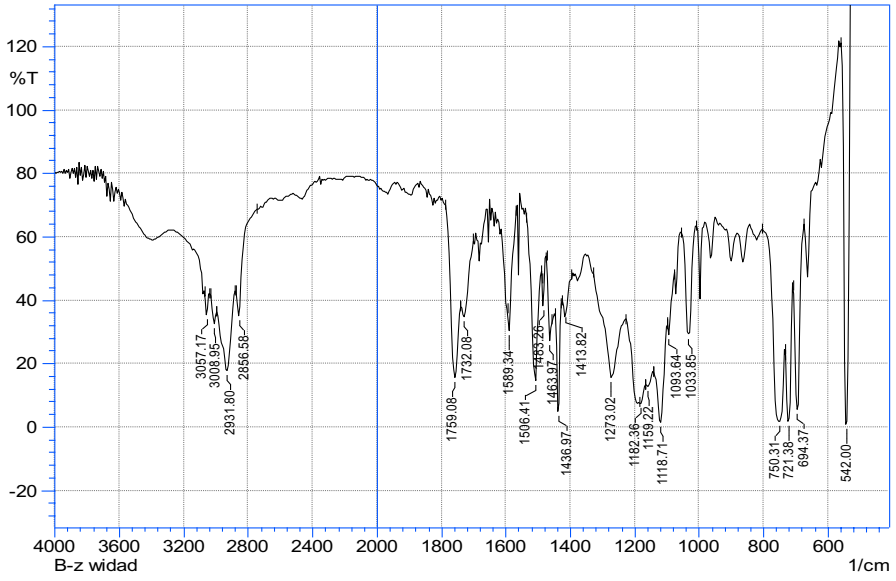


**Fig. 2** Fourier-transform infrared spectroscopy (FTIR) of m-PPV thin film

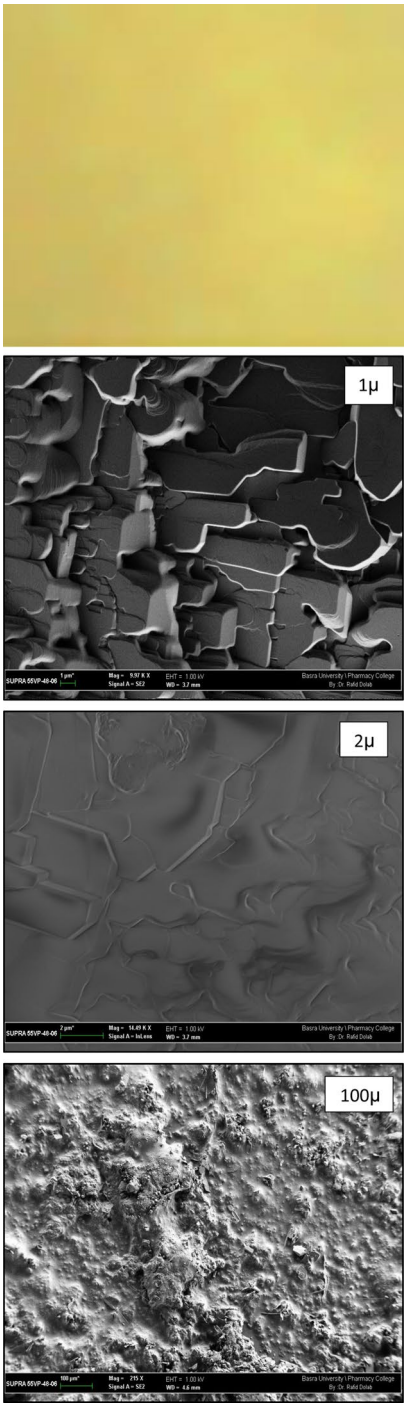


**Fig. 3** Photomicroscope and SEM image of m-PPV thin films

solution which survives the spin casting process and it persists into the film [28]. When the scale increases to 2μ and 1μ, a semi regular distribution of several plates appears, this aggregation of plates is maybe caused by agglomeration of the coiled chains [29].

## Optical properties

Optical characterizations of polymer such as optical absorption, transmission, luminescence spectra are the most important tools since they provide information about chemical and physical structures which are the configuration and conformation, respectively, of polymer chains [30]. Optical properties of the polymer depend on the properties of the solvent used to cast the film by modulating the aggregation state and conformation of the polymer chains. In this study, we use chloroform as solvent which is classified as a better one (in which a polymer can dissolve fully in a short time) [31].

### Absorption and energy gap

The UV–vis absorption is commonly used for studying the interactions between electrons and radiation, the spectral behavior of the optical absorbance of as-deposited and annealed thin film in the UV–vis range as shown in Fig. 4 which illustrates a sharp increase in absorbance toward UV region which is due to the fundamental absorption of light caused by excitation of electron from HOMO (highest occupied molecular orbital) to LUMO (lowest unoccupied molecular orbital); the redshift of the absorption edge of the annealed film resulted from formational change of the polymer chain as the annealing temperature higher than Tg of m-PPV, and the chains were relaxed, which led to the increasing of the chains length and caused this redshift. The absorption coefficient ($\alpha$) was calculated by using the relation

$$\alpha = 2.303A/t \tag{2}$$

The thickness of the film ($t$) ($5000 \pm 5$) Å was measured by using a micrometer with scale of 1 μm–1 cm The absorption data were manipulated for the calculation

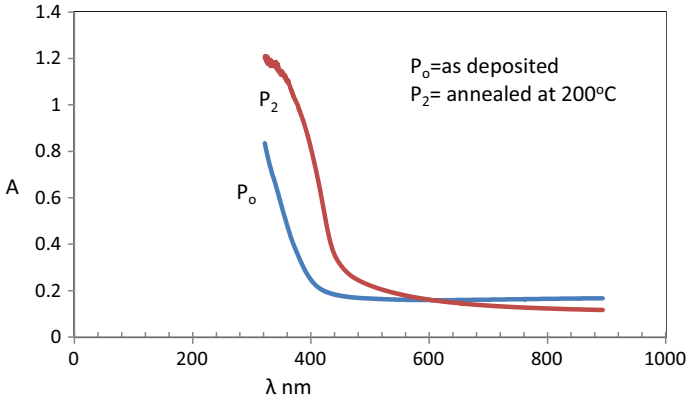


**Fig. 4** Absorption spectra of as-deposited and annealed m-PPV thin films

of the energy band gap. The energy band gap (in conjugated polymer) can be defined by the energy level splitting between the bonding (HOMO) and anti-bonding (LUMO) orbitals created between neighboring carbon orbitals ($\pi$–$\pi^*$) levels [32], the factor that influences the energy levels of electrons in polymer, and thus the ultimate band gap energy is the conjugation length which is referred to as the distance along the polymer chain with uninterrupted delocalization of molecular orbitals [33]. Figure 5 reveals the optical of energy gap as determined from the following relation [34].

$$\alpha hv = A\left(hv - E_{\mathrm{g}}\right)^{n} \tag{3}$$

where $A$ is constant and n assumes 1/2 in the case of allowed direct transition, since the absorption coefficient ($\alpha$) is more than $10^3$ for m-PPV deposited films. The calculated value of allowed energy gap (3.3 eV) of the ($\pi$–$\pi^*$) transition is consistent with the reported [19] but greater than the energy gaps of other derivatives of PPV [35], and the blue shift of band gap (with respect to other PPV derivatives) assigned to the shortening of the effective conjugation length due to the insertion of meta-linkage that influences the band gap, while the energy gap of the annealed film (2.85 eV) is redshifted with respect to as-deposited film; many factors may contribute to this redshift including relaxation of copolymer chains after annealing or molecular deformation elevation the degeneracy of the fundamental electronic transition. By introducing variation in polymeric structure, the energy gap of the ($\pi$–$\pi^*$) transition which is responsible for the color emitted is changed (Table 1).

The absorption coefficient in the exponential edge $\alpha < 10^{-4}$ cm$^{-1}$ can be evaluated from equation [36].

$$\alpha = \alpha_o \exp\left(hv/E_{\mathrm{u}}\right) \tag{4}$$

where $E_{\mathrm{u}}$ is the Urbach energy which is the width of band tail of the localized states in the band gap. Bond orders and polymer backbone kinks affect the electronic structure of polymer, the fluctuation of lattice configuration in polymer stain the

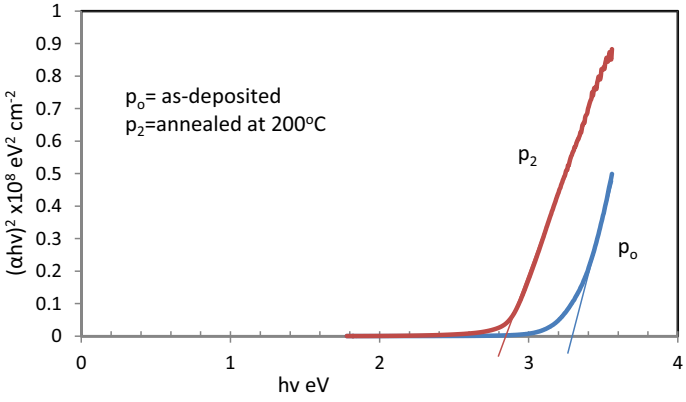


**Fig. 5** Direct energy band gap of as-deposited and annealed m-PPV thin films

**Table 1** XRD values of m-PPV thin films

| Tip width (°2Th.) | Rel. Int. (%) | d-spacing (Å) | FWHM (°2Th.) | Height (cts) | Pos. (°2Th.) |
|---|---|---|---|---|---|
| 0.1181 | 80.14 | 4.00531 | 0.0984 | 21.42 | 22.1949 |
| 0.0472 | 100 | 3.97338 | 0.0394 | 26.73 | 22.3756 |
| 0.2834 | 82.89 | 3.75466 | 0.2362 | 22.15 | 23.6974 |
| 3.0228 | 53.12 | 3.60664 | 2.519 | 14.2 | 24.685 |
| 0.3779 | 60.27 | 3.30395 | 0.3149 | 16.11 | 26.9873 |
| 0.0708 | 90.24 | 3.04807 | 0.059 | 24.12 | 29.3015 |
| 0.7557 | 44.21 | 2.83045 | 0.6298 | 11.82 | 31.611 |
| 0.1417 | 19.87 | 2.24349 | 0.1181 | 5.31 | 40.1968 |
| 0.1181 | 29.01 | 2.20044 | 0.0984 | 7.75 | 41.0181 |
| 0.4723 | 35.68 | 2.06181 | 0.3936 | 9.54 | 43.9143 |
| 0.2834 | 15.94 | 1.93925 | 0.2362 | 4.26 | 46.8496 |
| 0.1181 | 21.47 | 1.92178 | 0.0984 | 5.74 | 47.3013 |
| 0.6612 | 5.11 | 1.85039 | 0.551 | 1.36 | 49.2447 |
| 0.0945 | 20.01 | 1.82181 | 0.0787 | 5.35 | 50.07 |
| 0.2362 | 7.61 | 1.76126 | 0.1968 | 2.03 | 51.9167 |
| 0.1181 | 11.65 | 1.72176 | 0.0984 | 3.11 | 53.2003 |
| 0.1889 | 12.18 | 1.66478 | 0.1574 | 3.25 | 55.173 |
| 0.1417 | 21.83 | 1.64701 | 0.1181 | 5.83 | 55.8197 |
| 0.0945 | 9.41 | 1.62652 | 0.0787 | 2.52 | 56.586 |
| 0.2016 | 15.27 | 1.59432 | 0.168 | 4.08 | 57.7828 |

fundamental edge and produce the Urbach tail [37]. The Urbach tail of the absorption edge is usually ascribed to the optical electronic transitions between the excited states and the near edge localized states. In general, the Urbach energy represents the amount of disorder or structural defects in polycrystalline or amorphous materials [38]. By plotting Ln $\alpha$ versus $hv$ as shown in Fig. 6 for as-deposited and annealed meta-PPV films, the reciprocal slope of the linear part gives the value of $E_u$. The increase in the value of Urbach energy refers that the atomic structure disorder of films increases which leads to redistribution of states from band to tail. As a result, there would be a decrement in the optical band gap and an expansion of the Urbach tail taking place as seen in Table 2. $E_u$ values change inversely with the energy gap.

## Dispersion parameter

### Refractive index and dielectric constant

The optical constants are commonly determined from simultaneous measurement of absorbance and reflectance of the film material. Refractive index ($n$) (usually named dispersion) plays a vital role in optical devices designing, as it is decisive in all optical applications of transparent polymer, as it has a close relationship with the electronic polarization of ions and the local field inside the material; it is unique for each

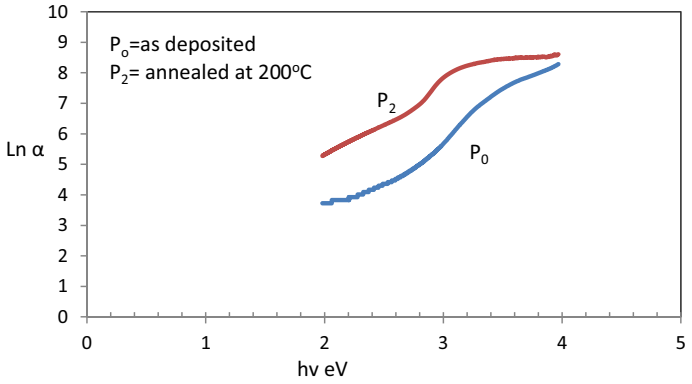


**Fig. 6** Plot of Ln $\alpha$ versus photon energy for as-deposited and annealed m-PPV films

**Table 2** Optical parameter values of m-PPV thin films

| Sample | $E_g$ (eV) | $E_u$ (eV) | $E_d$ (eV) | $E_o$ (eV) | $\epsilon_\infty$ | N/m* ($m^{-3}kg^{-1}$) | Stoke shift |
|---|---|---|---|---|---|---|---|
| As-deposited | 3.3 | 0.66 | 3.08 | 6.46 | 1,8 | $5\times10^{12}$ | 155 |
| Annealed | 2.85 | 1.53 | 0.86 | 3.78 | 195 | $7.5\times10^{12}$ | 126 |

material and may be utilized for both identification purposes and to predict other properties [39].

In the case of normal incidence and at range of frequencies in which absorption is weak $k^2 \ll (n-1)^2$, the of refractive index can be written as

$$n = 1 + R^{\wedge 1/2}/1 - R^{\wedge 1/2} \tag{5}$$

where $k$ is the extinction coefficient or attenuation constant which is measure part of the light lost due to scattering and absorption per unit distance calculated from $k=\alpha\lambda/4\pi$, the spectral dependence of refractive index appears in Fig. 7, and the change in refractive index indicates that some interactions take place between bands in polymeric material. The annealing process can increase the interchain interaction which leads to increase the dispersion hence increasing the refractive index, while the extinction coefficient increases toward higher photon energy corresponding to the beginning of strong electronic absorption and fraction of light lost due to scattering, as seen in Fig. 8; the extinction coefficient is related with α which increases with annealing. It appears that the redshift of each n and k, after thermal annealing, may be related to the variation in the conjugation length of the chains of the m-PPV.

The optical dielectric constant ($\epsilon_1$, $\epsilon_2$) is an essential intrinsic property of the material, and the real part of the dielectric constant reveals the amount by which it can decay the speed of light in the polymeric material; on the other hand, the imaginary part shows that a dielectric in the polymer absorbs energy from an electric field due to dipole motion [39]. The real and imaginary parts of the dielectric constant were calculated using the relations.

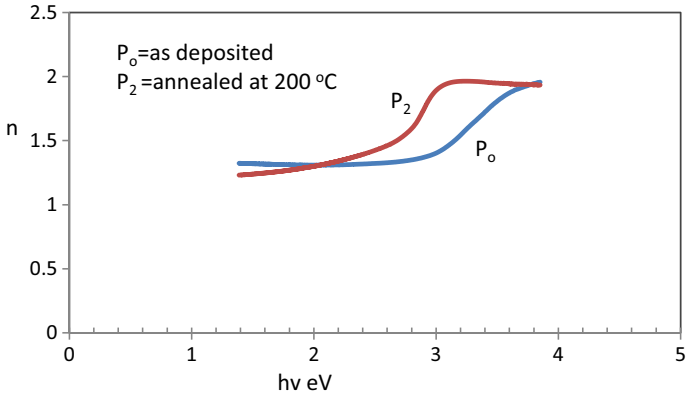


**Fig. 7** Refractive index spectra of as-deposited and annealed m-PPV thin films

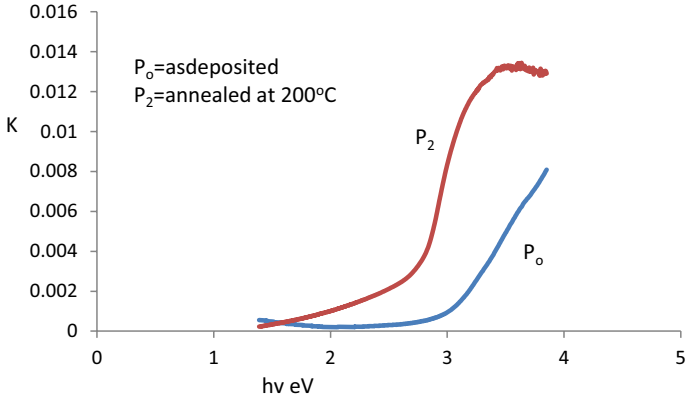


**Fig. 8** Extinction coefficient spectra of as-deposited and annealed m-PPV films

$$\epsilon_1 = n^2 - k^2 \qquad \epsilon_2 = 2nk \tag{6}$$

We can see that $\epsilon_1$ behaves similar to that of refractive index because of the smaller value of $k^2$ in comparison with $n^2$, while $\epsilon_2$ depends mainly on k values as seen in Figs. 9 and 10

## Dispersion energy parameters

The classical dispersion theory provides the description of refractive index in the region of very small value of extinction ($k$) under negligible damping. The high-frequency properties of thin films under investigation could be treated as single oscillator. The relation between the refractive index and single strength below the band gap in the transparent region is given by the relation [40].

$$\left(n^2 - 1\right) = E_o E_d / E_o^2 - (h\nu)^2 \tag{7}$$

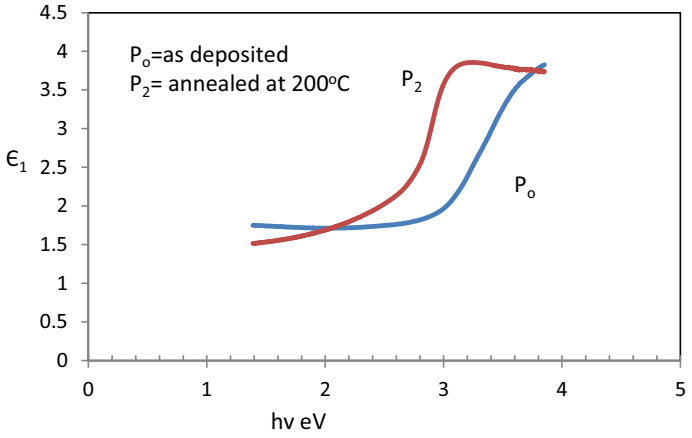


**Fig. 9** Real part of dielectric constant spectra of as-deposited and annealed m-PPV films

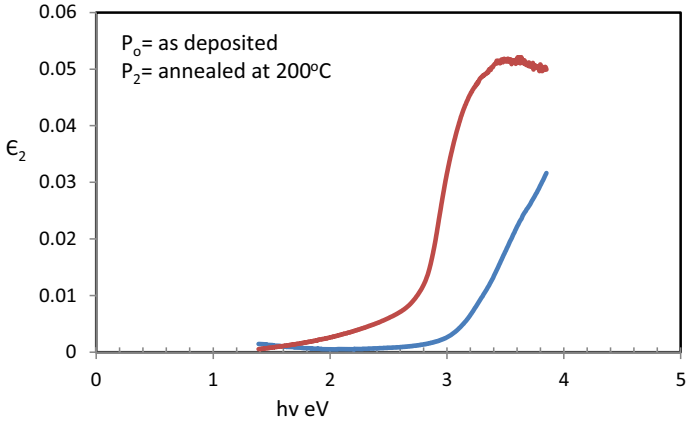


**Fig. 10** Imaginary part of dielectric constant spectra of as-deposited and annealed m-PPV films

$E_o$ is the energy of the oscillator which gives a quantitative information about the overall band structure of the material and corresponds to the distance between the center of the valance band and conduction band; it is therefore related to the band energy of different chemical bonds present in the molecules, and $E_d$ is the dispersion energy correlated to the average strength of the optical transition [41] which is a measure of the interband optical transition. This model describes the dielectric response for transitions below the optical gap, and $E_oE_d$ values were determined from slop $(E_oE_d)^{-1}$ and intercept $(E_oE_d)$ on the vertical axis of the plot $(n^2-1)^{-1}$ as a function of $(h\nu)^2$ as seen in Fig. 11.

### Complex dielectric constant near absorption edge

The analyzed data of refractive index ($n$) can be used to obtain the high-frequency dielectric constant ($\epsilon_\infty$) through the procedure, which represents the contribution of the free carriers and lattice vibrational modes of the dispersion [38].

$$\epsilon_1 = n^2 - k^2 = \epsilon_\infty - (e^2 N / 4\pi^2 C^2 \epsilon_o m^*)\lambda^2 \tag{8}$$

$\epsilon_1$ indicates to the real part of dielectric, $\epsilon_\infty$ is the lattice constant, $e$ is the charge of electron, $N$ is the free charge carrier concentration, $\epsilon_o$ is the permittivity of free space, $m^*$ is the effective mass of the electron, and C is the velocity of light. It is observed that the dependence of $\epsilon_1 = n^2$ on $\lambda^2$ is linear at longer wavelength as shown in Fig. 12, the extrapolating of the linear part to zero wavelength of the plot of $n^2$ versus $\lambda^2$ gives the values of $\epsilon_\infty$, and from the slop of the line we can calculate the value of $N/m^*$as seen in Table 2.

### Optical conductivity

The absorption coefficient and the refractive index can be used to calculate the optical conductivity ($\sigma_{opt}$) which is determined from the relation [38]

$$\sigma_{opt} = \alpha n C / 4\pi \tag{9}$$

where $C$ is the velocity of light; it is revealed from Fig. 13 that the optical conductivity follows the same manner as absorption coefficient and refractive index, and the increase in $\sigma_{opt}$ with increasing photon energy is due to high absorption of the film in that region. The increase in excited electron by photo energy after annealing was responsible for the high intensity of m-PPV thin film comparable to as-deposited film. The gradual increase in $\sigma_{opt}$ after (3 eV) for as-deposited film and (2.8 eV) for annealed film confirms the redshift of the absorbance after annealing.

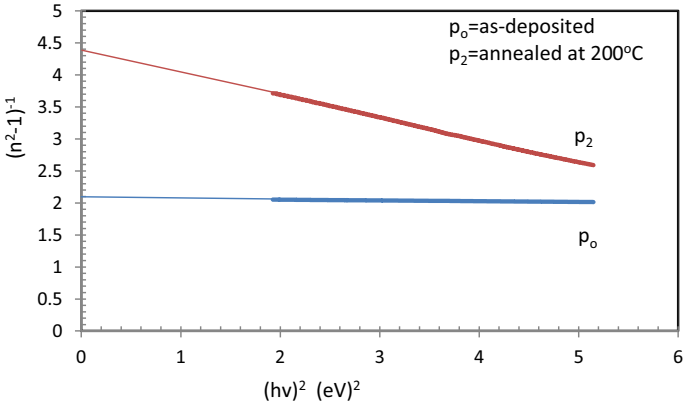


**Fig. 11** Variation in $(n^2-1)^{-1}$ as a function of $(h\nu)^2$ of as-deposited and annealed m-PPV films

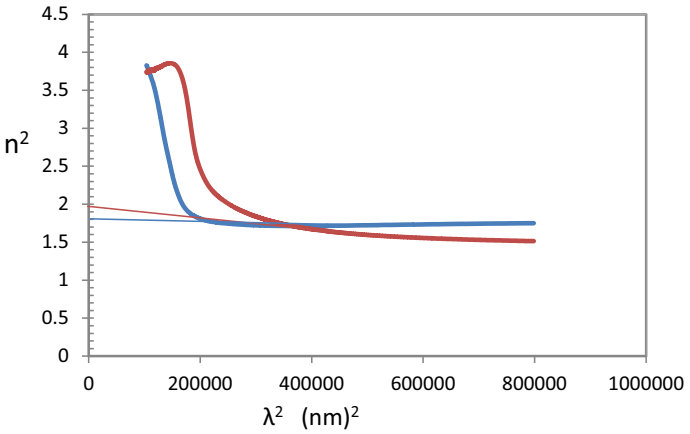


**Fig. 12** Variation in $n^2$ as a function of $\lambda^2$ of as-deposited and annealed m-PPV films

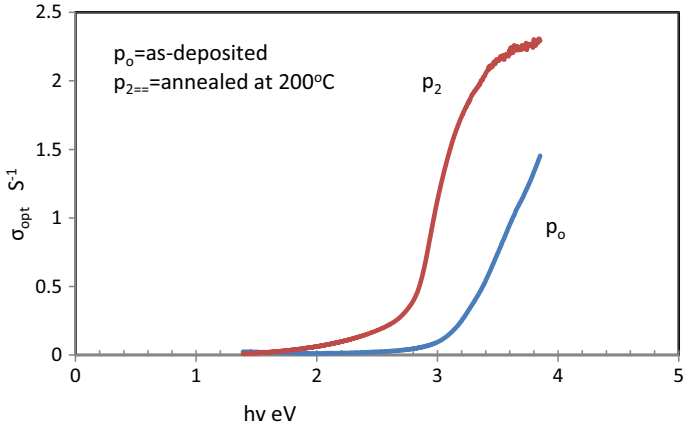


**Fig. 13** Optical conductivity spectra of as-deposited and annealed m-PPV films

## Photoluminescence (PL)

The photoluminescence (PL) emission in conjugated semiconductors is affected by stoichiometric defects in electronic levels. Photoluminescence measurement was taken with excitation wavelength at 350 nm for both as-deposited and annealed films. The PL will be redshifted from the absorption for any material, and the wave length separation between the peak of absorption and emission is known as stokes shift, since the absorption occurs from the lowest vibronic level of ground state and the emission occurs from the lowest vibronic level of the excited state; stokes shift is important in determining the energy loss through heating of an excited electron upon emission as well as the probability of an

emitted photon to be absorbed [33], and the reduction in apparent stokes shift after annealing interpreted increases in effective conjugation length [19].

The PL of polymer thin films was associated with chain conformation as well as interchain interaction in the films. Figure 14 shows the PL of meta-PPV for the as-deposited and annealed films both of which are attributing to emission characteristic of m-PPV backbone arises from relaxation of excited $\pi$-ê to the ground state. The insertion of meta-link significantly disrupts the conjugation along the polymer backbone with concomitant blue shifting of absorption and emission energies compared to other PPV derivatives based on p-xylene [42]. A noticeable reduction in intensity with a slight redshift can be seen after thermal annealing. The change in PL peak related with the increase in the conjugation length as a result of relaxation of polymer chain after annealing at temperature beyond $T_g$ (e.g. 200 °C) or during the annealing the oxygen might lead to carbonyl defects on polymer chain thus interrupting the conjugation, and the carbonyl acts a quenching sits and strongly affected the PL spectra [14]; on the other hand, the annealing process can increase the interchain interaction aggregation that leads to the reduction in PL efficiencies and redshift. In addition, the quenching of PL efficiencies indicates low-emission species that have been formed during the annealing, while increased flexibility of the polymer chain leads to a broadening of the spectrum.

## Conclusion

Thin films of m-PPV based on m-xylene were prepared by spin casting method on glass substrates. The effect of insertion meta-linkage on the structural and optical properties was studied. XRD results indicate polycrystalline structure with small peaks since meta-linkage reduces the crystallinity of the films. FTIR analysis confirms that the main chemical composition of m-PPV has been preserved. From optical measurements, the blue shift of allowed direct energy gap (3.3 eV) comparable

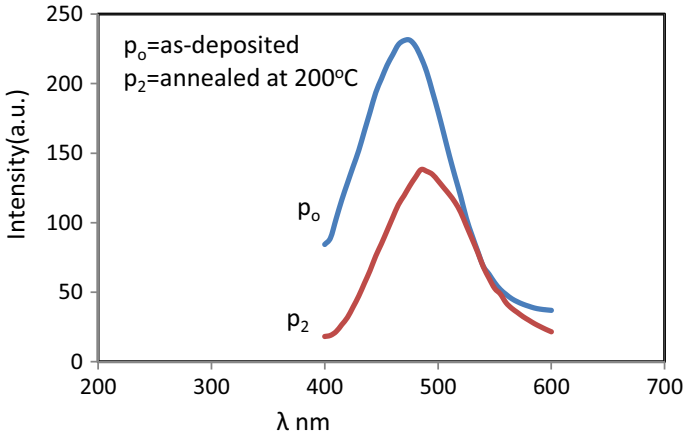


**Fig. 14** Photoluminescence spectra of as-deposited and annealed of m-PPV films

with other PPV derivatives assigned to the shortening of the effective conjugation length due to the influence of the meta-linkages on structure of copolymer and hence the optical properties. Thermal annealing affected the energy gap and related optical constant such as refractive index, extinction coefficient, dielectric constant, dispersion energy parameters, optical conductivity and photoluminescence spectra; several factors were responsible for the redshift including relaxation of polymer chains after annealing or during the annealing; the oxygen might lead to carbonyl defects on polymer chain thus interrupting the conjugation; furthermore, annealing process can increase the interchain interaction aggregation that leads to the reduction in PL efficiencies.

**Acknowledgements** The author would like to thank Dr. Widdad Hanoosh for his invaluable help in providing interaction materials and chemical analyses. And also the author wants to clarify that there is no conflict of interest with regard to potential sources of funding and conflict of interest (financial or non-financial), and there are no relationships or interests that can have a direct or potential impact or shift bias to work.

## References

1. Cambers DK, Karanam S, Qi D, Selmic S (2005) The electronic structure of oriented poly[2-methoxy-S-(2-ethyl-hexyloxy)-1,4-phenylene-vinylene]. Appl Phys A 80:483–488
2. Deng XY (2011) Light emitting devices with conjugated polymers. J Mol Sci 12:1573–1594
3. Burroughes JH, Bradley DD, Brown AR (1990) Light-emitting diodes based on conjugated polymers. Nature 347:539
4. Anikeeva PO (2009) Physical properties and design of light—emitting devices based on organic materials and nanoparticles. Thesis. Massachusetts Institute of Technology
5. Lee WH, Kong H, Oh SY (2009) Field effect transistors based on PPV derivatives as a semiconducting layer. Polym Chem 47:111–120
6. Mayer AC, Scully SR, Hardin BE, Rowell MW, McGehee MD (2007) Polymer-based solar cells. Mat Today 10:28–33
7. Jin Y, Kim J, Park SH (2005) Novel poly(p-phenylenevinylene)s derivatives with CF3-phenyl substituent for light-emitting diodes. Bull Korean Soc 26:855–858
8. Sreeram A, Patel NG, Venkatanarayanan RI (2014) Nanomechanical properties of poly(paraphenylene vinylene determined using quasi-static and dynamic Nano indentation. Polym Testing 37:86–93
9. Roncali (1997) Solitons in a box-the organic chemistry of electrically conducting polymers. J Chem Rev 97:173–205
10. Horst JWV (2001) The electronic and Optical properties of conjugated polymers predictions from first—principle solid state methods. Thesis. University Eindhoven, ISBN: 90-386-1769
11. Abdullah BA (2009) Synthesis and properties of some new PPV derivatives and their applications in PLEDs. Thesis. University of Basrah, pp 1–113
12. Cosslello RF, Akcelrud L, Atvars TD (2005) Solvent and molecular weight effects on fluorescence emission of MEH-PPV. J Braz Chem Soc 16:1678–4790
13. Bjorklund TG, Lin SH, Bardeen CJ (2004) The optical spectroscopy of poly(p-phenylene vinylene)/polyvinyl alcohol blends: from aggregates to isolated chromophores. Synth Metals 142:195–200
14. Shakoor A, Niaz NA, Majid A (2014) Opto-electronic properties of poly (p-phenylene vinylene) (PPV) intercalated in $CdPS_3$. Chalcogenide Lett 11:351–358
15. Chen JT, Hsu CS (2013) Poly(2,3-diphenyl-1,4-phenylenevinylene) (DP-PPV) derivatives: synthesis, properties, and their applications in polymer light-emitting diodes. Polymer 54:4045–4058
16. Farinola GM, Cardone A, Babudri F (2010) Fluorinated poly(p-phenylenevinylene)s: synthesis and optical properties of an intriguing class of luminescent polymers. Materials 3:3077–3091

17. Kim K, Jung MY, Zhong GL (2004) Morphology of poly(p-phenylenevinylene) thin films prepared directly on the surface of silicon wafers by the chemical vapor deposition polymerization. Synth Met 144:7–11
18. Massuyeau F, Arab H, Mihut L (2007) Optical properties of poly(para-phenylene vinylene) and single-walled carbon nanotube composite films: effects of conversion temperature, precursor dilution, and nanotube concentrations. J Phys Chem C 111:15111–15118
19. Akcelrud L (2003) Electroluminescent polymers. Prog Polym Sci 28:875–962
20. M-xylene International Chemical Safely Cards IPCS, NlOSH July (2014)
21. Liu J, Guo TF, Yang Y (2002) Effects of thermal annealing on the performance of polymer light emitting diodes. J Appl Phys 91:1595–1600
22. Thambidurai M, Murugan N, Muthukumarasamg N (2009) Preparation and characterization of nanocrystalline CdS Thin Films. Chalcogenide Lett 6:171–179
23. Ali HM, Mohamed HA, Wakked MM (2007) Properties of transparent conducting oxides formed from CdO alloyed with $In_2O_3$. Thin Solid Film 515:3024–3029
24. Sakthivel S, Boopathi A (2016) Structural and morphological characterizations of poly(P-Phenylene Vinylene) thin film by spin coating application of polymer LED. J Pure Appl Ind Phys 6:29–33
25. Mao WL, Mao H, Prokapenka VB (2006) The effect of pressure and volume of ferromagnesian post-perovskite. Geophys Res Lett 33:1–4
26. Bjorklund TG, Lin SH, Bardeen CB (2002) Dependence of poly(p-phenylene vinylene) morphology and time-resolved photophysics on precursor solvent. Synth Met 126:295–299
27. Schlick H, Stelzer F, Tasch S (2000) Highly luminescent poly(m-phenylene vinylene)-co- (p-phenylene vinylene) derivatives synthesized via metathesis condensation (ADMET). J. Macromol Catal 160:71
28. Juhari N, Majid WHA, Zainol AI (2013) The SEM & AFM images of MEH-PPV films below CLA Region. Procedia 53:354–361
29. Nguyen T-Q, Yee RJ, Schwartz BJ (2001) Solution processing of conjugated polymers: the effects of polymer solubility on the morphology and electronic properties of semiconducting polymer films. J Photochem Photobiol A Chem 144:21–30
30. Alias ZN, Zabid ZM, Ali AUM (2013) Optical characterization and properties of polymeric materials for optoelectronic and photonic applications. Int J Appl Sci Technol 3:11–38
31. Nguyen TP, Yang SH, Rendu PL (2005) Optical properties of poly(2-methoxy-5-(2′-ethylhexyloxy)-phenylene vinylene) deposited on porous alumina substrates. Compos Part A 36:515–519
32. Kagan J (1993) Organic photochemistry principle and application. Academic Press, Cambridge
33. Leger JM (2005) Electrochemical doping and the optical properties of light emitting polymer materials and devices. Thesis. University of California 2740
34. Jayasree Y, Pathi UC, Bhaskar PU (2012) Effect of precursor concentration and bath temperature on the growth of chemical bath deposited tin sulphide thin films. Appl Surf Sci 258:2732–2740
35. Omer BM (2012) Optical properties of MEH-PPV and MEH-PPV/ [6,6]-phenyl C61-butyric acid 3-ethylthiophene ester thin films. J Nano Electron Phys 4:04006-1–04006-4
36. Misra A, Kumar P, Srivastava R (2005) Electrochemical and optical studies of conjugated polymers for three primary colours. Indian J Pure Appl Phys 43:921–925
37. Alwan TJ, Mushtak A (2010) Structure and optical properties of CuAlS_2 thin films prepared via chemical bath deposition. Turk J Phys 34:107–116
38. Skettrupt T (1978) Urbach's rule derived from thermal fluctuations in the band-gap energy. Phys Rev B 18:2622–2631
39. Hafiz MM, Elkabany N, Koth HM (2015) Determination of optical band gap and optical constants of $Ge_xSb_{40-x}Se_{60}$ thin films. Int J Thin Films Sci Technol 3:179–185
40. El-Nahass MM, Afify HA, Gadallah AS (2014) Effect of thermal annealing on structural and optical properties of titanyl phthalocyanine thin films. Mater Sci Semicond Process 27:254–260
41. Oboudi SF, Abdul Nabi MT, Al-Taay WA (2015) Dispersion characterization of conductive polymer. Int J Electrochem Sci 10:1555–1562
42. Farinola GM, Cardone A, Babudri F (2010) Fluorinated poly(p-phenylenevinylene)s: synthesis and optical properties of an intriguing class of luminescent polymers. Materials 3:3077–3091